Geochimica et Cosmochimica Acta, Vol. 69, No. 6, pp. 1575–1588, 2005

0016-7037/05 $30.00 + .00

doi:10.1016/j.gca.2004.09.029

Dissolution of cinnabar (HgS) in the presence of natural organic matter

JACOB S. WAPLES,[1] KATHRYN L. NAGY,[1,*] GEORGE R. AIKEN,[2] and JOSEPH N. RYAN[3]

[1]Department of Geological Sciences, 399 UCB, University of Colorado, Boulder, CO 80309, USA
[2]United States Geological Survey, Water Resources Division, 3215 Marine Street, Boulder, CO 80303, USA
[3]Department of Civil, Environmental, and Architectural Engineering, 428 UCB, University of Colorado, Boulder, CO 80309, USA

(*Received December* 22, 2003; *accepted in revised form September* 29, 2004)

Abstract—Cinnabar (HgS) dissolution rates were measured in the presence of 12 different natural dissolved organic matter (DOM) isolates including humic, fulvic, and hydrophobic acid fractions. Initial dissolution rates varied by 1.3 orders of magnitude, from 2.31×10^{-13} to 7.16×10^{-12} mol Hg (mg C)$^{-1}$ m^{-2}s^{-1}. Rates correlate positively with three DOM characteristics: specific ultraviolet absorbance ($R^2 = 0.88$), aromaticity ($R^2 = 0.80$), and molecular weight ($R^2 = 0.76$). Three experimental observations demonstrate that dissolution was controlled by the interaction of DOM with the cinnabar surface: (1) linear rates of Hg release with time, (2) significantly reduced rates when DOM was physically separated from the surface by dialysis membranes, and (3) rates that approached constant values at a specific ratio of DOM concentration to cinnabar surface area, suggesting a maximum surface coverage by dissolution-reactive DOM. Dissolution rates for the hydrophobic acid fractions correlate negatively with sorbed DOM concentrations, indicating the presence of a DOM component that reduced the surface area of cinnabar that can be dissolved. When two hydrophobic acid isolates that enhanced dissolution to different extents were mixed equally, a 20% reduction in rate occurred compared to the rate with the more dissolution-enhancing isolate alone. Rates in the presence of the more dissolution-enhancing isolate were reduced by as much as 60% when cinnabar was prereacted with the isolate that enhanced dissolution to a lesser extent. The data, taken together, imply that the property of DOM that enhances cinnabar dissolution is distinct from the property that causes it to sorb irreversibly to the cinnabar surface.

1. INTRODUCTION

Interactions of mercury (Hg) in aqueous, particulate, and mineral forms with dissolved organic matter (DOM) play important roles in controlling reactivity, bioavailability and transport of Hg(II), in aquatic systems (Ravichandran, 2004). Several investigators have proposed DOM complexation of Hg(II) as a primary mechanism for the transport of mercury (Meili, 1991; Krabbenhoft and Babiarz, 1992; Driscoll et al., 1994; Shanley et al., 2002) based on a strong correlation between dissolved mercury and dissolved organic carbon (DOC) concentrations in ground, lake, and stream waters. The strongest binding sites for Hg(II) on DOM are reduced sulfur functional groups as determined from synchrotron X-ray absorption spectroscopic measurements (Xia et al., 1999; Skyllberg et al., 2000; Hesterberg et al., 2001) and binding experiments (Benoit et al., 2001; Haitzer et al., 2002; Hsu and Sedlak, 2003; Lamborg et al., 2003). Weaker binding to oxygen functional groups such as carboxyls (Reddy and Aiken, 2001) occurs only at relatively high mercury concentrations, atypical of most natural settings.

Formation of relatively insoluble solid mercury sulfides (HgS), cinnabar or metacinnabar (Martell and Smith, 1998), can inhibit Hg(II) methylation and bioaccumulation (Compeau and Bartha, 1987), and immobilize mercury Hg(II) in sediments. However, the presence of DOM enhances the solubility and dissolution of cinnabar (Ravichandran et al., 1998), which lessens the role of cinnabar in immobilizing Hg(II). DOM also inhibits the precipitation of metacinnabar (Ravichandran et al., 1999), which is conceptually consistent with the dissolution enhancement. In contrast to the spectroscopic evidence that reduced sulfur sites on DOM bind mercury most strongly, enhancement of cinnabar dissolution appears to be correlated with aromaticity, and not the sulfur content, of the DOM based on a limited number of DOM samples from the Florida Everglades examined by Ravichandran et al. (1998).

The interaction between DOM and cinnabar in both promoting dissolution and enhancing aqueous Hg solubility contrasts with observations of the interactions between humic substances and metal oxides. Whereas strong binding of DOM to a dissolved cation generally accounts for the mobility of metals in the aqueous phase of the natural environment, there is no simple relationship between humic substances and oxide mineral dissolution rates despite the fact that low molecular weight organic ligands tend to promote oxide mineral dissolution in the laboratory (Hering, 1995). Furthermore, interactions of DOM with oxide mineral surfaces also can remove DOM and metals from solution via sorption (Jardine et al., 1989; McKnight et al., 1992) and inhibit solid dissolution and precipitation (Hering, 1995). Processes that control sorption interactions of DOM with mineral surfaces are complex with evidence for hysteresis (Gu et al., 1994), different sorption affinities (Davis, 1982; Jardine et al., 1989; Gu et al., 1995; Wang et al., 1997), and competition among different DOM fractions (Ochs et al., 1994; Gu et al., 1996).

We describe the results of experiments on the interactions of

* Author to whom correspondence should be addressed, at Department of Earth and Environmental Sciences, University of Illinois at Chicago (MC-186), 845 West Taylor Street, Chicago, IL 60607-7059, USA (klnagy@uic.edu).
† *Present address:* Golder Associates Inc., 44 Union Blvd., Suite 300, Lakewood, CO USA 80228.

Table 1. Site descriptions for aquatic organic matter isolates.

Sample	Site description
Suwannee River Humic Acid (SRHA) Suwannee River Fulvic Acid (SRFA)	Black water river draining the Okeefenokee Swamp. Sampled at Fargo, Georgia. Vegetation types: Southern Floodplain Forest (Quercus, Nyassa, Taxodium); International Humic Substances Society standards.
Ogeechee River Humic Acid (OgRHA) Ogeechee River Fulvic Acid (OgRFA)	Small river draining the Piedmont in Eastern Georgia. Sampled at Grange, Georgia. Vegetation types: Oak-Hickory-Pine Forest (Quercus, Carya, Pinus).
Coal Creek Fulvic Acid (CCFA)	Small mountain stream draining the Flattops Wilderness Area, Colorado. Vegetation type: Spruce-Fir Forest (Picea, Abies).
F1 Hydrophobic Acid (F1HpoA)	Eutrophied marshland located in Water Conservation Area 2A in the northern Everglades. Vegetation dominated by cattails. (26°21′35″ N; 80°22′14″ W).
2BS Hydrophobic Acid (2BSHpoA)	Relatively pristine marshland located in Water Conservation Area 2B in the northern Everglades. Vegetation dominated by saw grass. (26°09′00″ N; 82°22′30″ W).
Ohio River Fulvic Acid (OhRFA)	Major river draining east-central United States. Sampled at Cincinnati, Ohio. Vegetation types: Appalachian Oak Forest, Mixed Mesophytic Forest, Oak Hickory Forest.
Missouri River Fulvic Acid (MRFA)	Major river draining north-central United States. Sampled at Sioux City, Iowa. Vegetation types: Northern Floodplain Forest and Wheatgrass, Needlegrass, and Bluestem Grasslands.
Pacific Ocean Fulvic Acid (POFA)	Sample collected from 100 m depth, 170 km southwest of Honolulu, Hawaii, Marine organic matter.
Lake Fryxell Fulvic Acid (LFFA)	Ice-covered lake in the McMurdo Dry Valleys, Antarctica. Organic matter dominated by autochthonous sources (algae, bacteria).
Williams Lake Hydrophobic Acid (WLHpoA)	Seepage lake in north-central Minnesota. Organic matter dominated by autochthonous sources (algae, bacteria, emergent vegetation).

cinnabar with 12 samples of DOM obtained from a variety of aquatic systems and having a wide range in chemical composition and reactivity. The goals were to quantify the rate of cinnabar dissolution as a function of DOM composition and determine the role of sorption of DOM onto cinnabar in the dissolution mechanism. The results are important for understanding the dynamics of Hg-cycling in the environment, including sites heavily contaminated with Hg such as at Oak Ridge, TN (Barnett et al., 1997), sites that contain naturally occurring or mined deposits of cinnabar (Covelli et al., 2001), sites where cinnabar-containing sediments are transported to organic-rich water bodies such as the Sacramento River and the Sacramento-San Joaquin delta in California (Domagalski, 2001), and sites containing sulfide and atmospherically deposited mercury, such as the Florida Everglades (Hurley et al., 1998; Benoit et al., 1999; Krabbenhoft et al., 2000).

2. MATERIALS AND METHODS

2.1. Materials

Certified A.C.S. or trace-metal grade reagents and deionized (DI) water (>18.0 MΩ; DOC < 0.2 mg C L^{-1}) were used. Glassware was cleaned with 10 wt% NaOH to remove DOM, and an aqua regia solution (three parts concentrated HCl, one part concentrated HNO_3, and two parts water) to remove cinnabar and mercury, and then rinsed at least 15 times with DI water.

Powdered cinnabar (HgS_{red}), 99.5+% (Acros Organics), was soaked in HNO_3 (10% by volume) for 3 d and then rinsed with 100 mL aliquots of DI water until a pH of 6 to 7 was measured for at least 10 successive rinses. For each rinse, the mixture was stirred vigorously with a glass rod and then left to settle for 2 min. Fine suspended particles were removed by decanting. Cinnabar was oven-dried at 60°C and then sieved (30–70 μm fraction) using Spectra/Mesh nylon filters. X-ray diffraction (Scintag PADV powder diffractometer with graphite beam monochrometer; Cu-Kα radiation; 10° to 80° 2θ at 2° 2θ min^{-1}) was used to confirm mineral purity. A surface area of 0.23 m^2 g^{-1} was measured by BET N_2 adsorption (Gemini 2360). Scanning electron microscopy (SEM; ISI SX-30) showed particles of irregular shape varying in maximum dimension from about 2 to 40 μm.

Natural organic matter (NOM) isolates in freeze-dried form were obtained from a variety of environments (Table 1) using methods described by Aiken et al. (1992). NOM isolates were characterized by determining elemental composition (Huffman and Stuber, 1985), molecular weight by high-pressure size exclusion chromatography (HPSEC) (Chin et al., 1994), specific ultraviolet (UV) light absorbance (Weishaar et al., 2003), and by ^{13}C-NMR spectroscopy (Wershaw, 1985) (Table 2). Select samples were examined for sulfur speciation using X-ray absorption spectroscopy (XANES) (Vairavamurthy et al., 1997) (Table 2).

Dried NOM isolates were dissolved in 0.01 M $NaNO_3$ and the solutions were adjusted to pH 6.0 (±0.2) using either NaOH or HNO_3 while in contact with the atmosphere. DOC concentrations were determined using Oceanography International Model 700 and 1010 carbon analyzers. UV light absorbance measurements were made with a Hewlett-Packard 8453 spectrophotometer. Specific UV absorbance at 280 nm ($SUVA_{280}$), an indicator of the degree of aromaticity (Weishaar et al., 2003), was determined for each DOM isolate solution as:

$$\left(\frac{\text{UV absorbance}}{\text{DOC}}\right) = \text{SUVA}_{280} \quad (1)$$

where UV absorbance is expressed as absorbance per cm of path length and DOC concentration is in mg C L^{-1}. Errors in $SUVA_{280}$ values were calculated using an error of ±0.005 absorbance units for the UV absorbance measurement and the standard deviation between duplicate measurements for the DOC concentration. Values of $SUVA_{280}$ for the DOM solutions in 0.01 M $NaNO_3$ were corrected for interfering absorbance (with a peak absorbance observed at 207 nm) from a solution of 0.01 M $NaNO_3$. Average values for $SUVA_{280}$ errors were ±0.0020 for solutions from the standard dissolution experiments and ±0.0010 for solutions from sorption isotherm measurements using F1HpoA and WLHpoA. The difference in errors is a function of the two different instruments used for the DOC analyses.

2.2. Experimental Methods

2.2.1. Dissolution Experiments

In batch experiments, cinnabar was reacted with one isolate (standard dissolution experiment), two isolates (mixture experiment), or prereacted with one isolate before reacting with a second isolate that was added to or replaced the first isolate (prereacted mixture and prereacted replacement experiments, respectively). Control experiments also were carried out: pure water, 0.01 M $NaNO_3$, 10 g L^{-1} HgS(s) in 0.01 M $NaNO_3$, and DOM in 0.01 M $NaNO_3$.

All experiments were conducted at 22 ± 1°C in 125 mL glass

Table 2. Chemical characteristics of DOM isolates.[a]

DOM	C (wt%)	H (wt%)	O (wt%)	N (wt%)[e]	S (wt%)	Ash (wt%)	MW[b] (Da)	Aliphatic I (0–62 ppm)	Aliphatic II (62–90 ppm)	Acetal (90–110 ppm)	Aromatic (110–160 ppm)	Carboxyl (160–190 ppm)	Ketone (190–230 ppm)	Reduced S[d] (mol% total S)	$SUVA_{280}$[c] L $(mg\ C)^{-1}\ cm^{-1}$
SRHA[f]	53.4	3.9	40.9	1.1	0.68	4.13	1399[f]	21.3	7.3	6.6	35.1	20.7	9.0	18.3[g]	0.0547
OgRHA	54.6	4.9	36.8	1.6	1.8	3.9	1906[h]	24.7	10.4	7.3	40.8	15.1	1.6	19.5	0.0528
OgRFA[h]	54.0	4.02	38.5	0.93	1.27	0.39	1021[h]	33.0	13.9	6.8	24.7	18.3	3.3	22.6	0.0289
CCFA[h]	52.8	4.5	38.4	0.95	0.7	1.23	1180[i]	34.7	8.1	1.6	28.0	23.1	4.5	15.7	0.0330
F1HpoA[f]	52.2	4.64	39.9	1.53	1.73	9.37	1031	33.1	8.9	2.3	25.4	23.1	7.2	28.7[g]	0.0309
SRFA[f]	54.2	3.92	38.0	0.72	0.35	0.19	1360[j]	35.0	10.1	5.0	22.9	21.3	5.6	16.6[g]	0.0301
2BSHpoA[f]	52.3	4.79	40.2	1.58	1.23	7.31	953	39.5	9.2	1.6	21.3	22.2	6.3	30.4[g]	0.0227
OhRFA	55.5	5.4	35.9	1.5	1.28	0.57	705[k]	33.6[k]	15.2[k]	5.6[k]	24.3[k]	19.3[k]	1.6[k]	22.4	0.0217
MRFA[h]	55.4	5.3	35.0	1.3	0.78	0.1	839[l]	40.0	11.9	4.5	20.4	18.8	4.4	19.6	0.0184
POFA	56.2	6.0	36.3	1.1	0.4	0.36	532[h]	56.9	13.4	1.2	7.3	19.5	1.6	12.5	0.0044
LFFA[l]	55.0	5.5	34.9	3.3	1.2	2.3	468	46.4	14.5	4.4	15.2	19.6	0	nd	0.0141
WLHpoA	52.7	5.2	36.6	1.7	0.72	2.98	772[h]	50.0	15.0	5.8	13.8	13.9	1.5	nd	0.0132

[a] Data sources identified by superscript next to DOM acronym, unless otherwise noted.
[b] Number-average molecular weight (Cabaniss et al., 2000).
[c] Values determined in this study according to Eqn. 1.
[d] Sum of thiol and polysulfide functional groups as obtained from XANES data (Vairavamurthy et al., 1997).
[e] Elemental concentrations are reported on an ash-free basis.
[f] Ravichandran et al. (1998).
[g] Ravichandran (1999).
[h] Y. Chin, Ohio State University.
[i] Chin et al. (1997).
[j] Chin et al. (1994).
[k] Data for this sample were unavailable; data taken from another OhRFA sample collected. July 1999.
[l] Aiken et al. (1996).

Erlenmeyer flasks with ground-glass stoppers. Cinnabar was added prior to the isolate solutions, after which the flasks were stoppered, sealed with electrical tape, placed in thick foam containers, and rotated end-over-end at 4 rpm on a rotator consisting of an electric motor and wheel. Experiments were performed in triplicate, with a fourth control flask containing only DOM solution. Four samples were taken from each flask during the first 10 h of reaction. After 10 h, one of the triplicate flasks was removed for analysis of DOM concentration and not sampled again. Experiments beyond 10 h were completed in duplicate and sampled at 25 h. The pH was measured at each sampling and adjusted, if necessary, to 6.0 ± 0.2 with 0.01 M NaOH or HNO_3.

Placement of the flasks in the foam containers blocked fluorescent laboratory light (there was no sunlight) from the experiments. In a separate test conducted to determine the potential for photooxidation of DOM in the presence of $NaNO_3$, a flask containing 10 mg C L^{-1} of F1HpoA and 0.1 M $NaNO_3$ was exposed to laboratory light on the bench top for 15 d.

Flasks were removed from the rotator and the contents settled for 5 min before removing solution for analysis. For Hg analyses, 3 to 15 mL of solution were extracted using a disposable polypropylene syringe and filtered through a 0.1 μm PTFE membrane (Whatman Puradisc) previously wetted with isopropanol (99.9%) and rinsed with 30 mL of water. The first milliliter of filtrate was discarded. The filtrate was oxidized with 15 mL of 5 wt% potassium permanganate and 8 mL of 5 wt% potassium persulfate at 90°C to convert all Hg to uncomplexed Hg(II). Excess permanganate and persulfate were reduced with 6 mL of 12 wt% hydroxylamine chloride in 12 wt% sodium chloride. Hg(II) was reduced to Hg^0(g) with 5 mL of 10 wt% stannous chloride in 0.1 N sulfuric acid. Mercury content was determined using cold vapor atomic adsorption spectrophotometry (CVAAS) (Buck Scientific model 400A) with a detection limit of 0.05 μg. For the DOC and UV absorbance analyses, conducted in duplicate, approximately 17 mL of sample were removed with a polypropylene syringe and filtered through a 0.1 μm Supor membrane (Pall Acrodisc). Sulfur released to solution was not measured.

All dual isolate experiments were conducted using solutions of Williams Lake (WLHpoA) and Florida Everglades F1 (F1HPoA) hydrophobic acids. In the mixture experiment, WLHpoA and F1HPoA solutions were combined in approximately equal parts before adding to the cinnabar. In the prereacted mixture experiments, 63 mL of a DOM solution were equilibrated with cinnabar while rotating for approximately 2.5 h. After this equilibration step, a fresh DOM solution of equal volume and concentration was added and the experiment continued. In the prereacted replacement experiments, 125 mL of a solution containing about 10 mg C L^{-1} of either WLHPoA or F1HPoA equilibrated with cinnabar while rotating for 2.5 h. After stopping and allowing the cinnabar to settle for 30 to 40 min, the supernatant was decanted through a 0.45 μm Millipore Durapore membrane HV filter in a PTFE filter apparatus. Fresh DOM solution was then added to the cinnabar to make a total volume of 125 mL and the experiment was continued. Approximately 2% of the HgS was lost during decanting as determined by mass difference on the dried filter. This corresponds to a maximum decrease in surface area of 3.5%, assuming that all filtered particles were 2 μm in diameter.

In all experiments, dissolved Hg was normalized to DOM concentration, cinnabar surface area (0.23 m^2 g^{-1}), solution volume (0.125 L), and cinnabar concentration (generally 10 g L^{-1}). Cinnabar dissolution rates (mol Hg (mg C)$^{-1}$ m^{-2} s^{-1}) were determined from the slopes of linear regressions of normalized Hg concentration released versus time including the point (0,0). The calculated uncertainty of the slopes ranged from 2.1 to 14.2%.

2.2.2. *Dialysis Experiments*

Approximately 20 cm lengths of dialysis tubing composed of cellulose ester membranes (15 mm diameter) with a molecular weight cutoff of 1000 Da (Spectra Por) were rinsed three times and then soaked in water overnight to remove the sodium azide storage solution. The tubing was tied at both ends to form bags with volumes of 7 mL. Interior solutions contained 20 mg C L^{-1} of the F1HpoA isolate. Both interior and exterior solutions contained 0.01 M $NaNO_3$ at pH 6.0 (±0.2) and 5×10^{-4} M KBr. The KBr was added to facilitate transport of Hg through the membrane (Haitzer et al., 2002). Three control experiments were performed: one without KBr, one without DOM, and one without HgS.

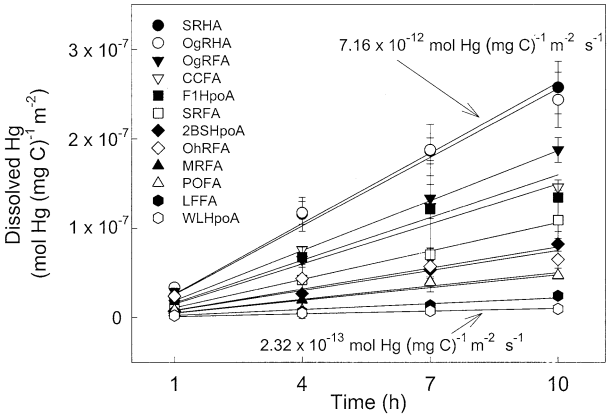

Fig. 1. Concentrations of Hg released from cinnabar exposed for 10 h to 12 different DOM isolates. Concentrations are normalized to the initial DOM concentrations (approximately 10 mg C L^{-1}) and the total surface area of the cinnabar (10 g HgS L^{-1}).

Cinnabar (1.0 g), DOM-free solution (93 mL), and the filled dialysis bag were placed in a 125 mL glass jar with a PTFE-lined screw cap, which was then rotated for up to 9 d. Interior and exterior solutions were analyzed for Hg, DOC, and UV absorbance. Dissolved Hg was measured with a cold vapor atomic fluorescence spectrometer (CVAFS) (detection limit of 0.1 ng L^{-1}) in the control experiments. For this analysis, DOM and Hg were oxidized using a solution of 0.03 M potassium bromate in 0.2 M potassium bromide. Excess bromate was reduced with a 1.35 M hydroxylamine hydrochloride solution. Mercury(II) was reduced using 2 wt% $SnCl_2$.

2.2.3. *Sorption Experiments*

The DOM sorbed to cinnabar in the standard dissolution experiments was quantified as the difference in DOM concentration between one of the triplicate flasks and the DOM blank after 10 h of reaction. Sorption as a function of total cinnabar surface area was measured for the WLHpoA and F1HpoA isolates using approximately 10 mg C L^{-1} solutions and cinnabar concentrations of 2 to 80 g HgS L^{-1} (0.46 to 18.4 m^2 HgS L^{-1}). Experiments were conducted as standard dissolution experiments and analyzed at 1 and 24 h. Sorbed DOM concentrations were determined by difference with concentrations in blank experiments lacking cinnabar. Sorption isotherms were measured for F1HpoA and WLHpoA at concentrations from approximately 2 to 16 mg C L^{-1} onto 2.3 m^2 L^{-1} HgS (10 g L^{-1} HgS) at pH 6.0 ± 0.2. DOM analyses were determined after 10 h for the F1HpoA isolate and after 23 h for WLHpoA. The amount of sorbed DOM was determined by difference between experiments with and without cinnabar.

3. RESULTS

3.1. Dissolution Rates in the Presence of Single DOM Isolates

Initial dissolution rates, calculated from data collected up to 10 h, varied by 1.3 orders of magnitude, from 2.32×10^{-13} mol Hg (mg C)$^{-1}$ $m^{-2}s^{-1}$ in solutions of WLHpoA to 7.16×10^{-12} mol Hg (mg C)$^{-1}$ $m^{-2}s^{-1}$ in solutions of Suwannee River Humic Acid (SRHA) (Fig. 1; Table 3). Rates were linear through 25 h of dissolution. The amounts of mercury released (about 10^{-8} M Hg) were 12 to 13 orders of magnitude higher than that for cinnabar in equilibrium with water (about 7×10^{-20} M Hg) based on thermodynamic calculations and

Table 3. Experimental conditions and cinnabar dissolution rates in standard dissolution experiments.[a]

Cinnabar concentration (g HgS L^{-1})	DOM	DOM concentration (mg C L^{-1})	10 h dissolution rate (mol Hg (mg C)$^{-1}$ m^{-2} s^{-1})	10 h dissolution rate (mol Hg $m^{-2}s^{-1}$)
10	SRHA	8.8	$7.31(0.16) \times 10^{-12}$	—
10	OgRHA	7.9	$7.12(0.28) \times 10^{-12}$	—
10	OgRFA	9.9	$5.19(0.18) \times 10^{-12}$	—
10	CCFA	9.9	$4.43(0.27) \times 10^{-12}$	—
10	F1HpoA	9.2	$4.15(0.30) \times 10^{-12}$	—
10	SRFA	9.6	$2.94(0.06) \times 10^{-12}$	—
10	2BSHpoA	9.6	$2.18(0.08) \times 10^{-12}$	—
10	OhRFA	10.4	$2.08(0.30) \times 10^{-12}$	—
10	MRFA	10.7	$1.39(0.08) \times 10^{-12}$	—
10	POFA	11.1	$1.32(0.16) \times 10^{-12}$	—
10	LFFA	9.2	$6.05(0.05) \times 10^{-13}$	—
10	WLHpoA	9.7	$2.76(0.02) \times 10^{-13}$	—
10	F1HpoA	2.3	$4.89(0.25) \times 10^{-12}$	$1.12(0.06) \times 10^{-11}$
10	F1HpoA	4.8	$5.27(0.47) \times 10^{-12}$	$2.53(0.23) \times 10^{-11}$
10	F1HpoA	7.4	$4.16(0.12) \times 10^{-12}$	$3.08(0.09) \times 10^{-11}$
10	F1HpoA	9.3	$4.12(0.29) \times 10^{-12}$	$3.83(0.27) \times 10^{-11}$
10	F1HpoA	18.3	$2.05(0.11) \times 10^{-12}$	$3.75(0.20) \times 10^{-11}$
10	F1HpoA	35.5	$1.14(0.05) \times 10^{-12}$	$4.05(0.16) \times 10^{-11}$
20	F1HpoA	5.3	$4.75(0.36) \times 10^{-12}$	$1.26(0.10) \times 10^{-11}$
20	F1HpoA	9.1	$4.21(0.57) \times 10^{-12}$	$1.92(0.26) \times 10^{-11}$
20	F1HpoA	14.0	$3.86(0.21) \times 10^{-12}$	$2.70(0.15) \times 10^{-11}$
20	F1HpoA	18.4	$4.00(0.38) \times 10^{-12}$	$3.68(0.35) \times 10^{-11}$
20	F1HpoA	36.8	$2.30(0.13) \times 10^{-12}$	$4.23(0.23) \times 10^{-11}$
20	F1HpoA	73.2	$1.19(0.07) \times 10^{-12}$	$4.36(0.24) \times 10^{-11}$

[a] Numbers in parentheses are 2 standard deviations.

assuming stoichiometric dissolution. Mercury release was below detection in all control experiments.

Dissolution rates correlate strongly with $SUVA_{280}$ ($R^2 = 0.88$), aromaticity ($R^2 = 0.80$), and molecular weight (MW) ($R^2 = 0.76$) (Fig. 2, Table 4) of the DOM isolates. Aromaticity is internally correlated with both molecular weight and $SUVA_{280}$ (Chin et al., 1994), therefore these three variables were not cross-correlated. No relationship was observed between dissolution rate and total or reduced sulfur content. Correlations of rate with $SUVA_{280}$ and any other chemical characteristic of the DOM are not significantly better than those with $SUVA_{280}$ alone (Table 4).

The release rate of Hg (mol Hg m^{-2} s^{-1}) from cinnabar increased with increasing F1HpoA concentration up to a threshold value for the ratio of DOM concentration to cinnabar surface area above which the rate was relatively constant (Table 3, Fig. 3). The threshold ratios were 0.92 (9.3 mg C L^{-1} with 10 g L^{-1} HgS) and 0.93 (18.4 mg C L^{-1} for 20 g L^{-1} HgS). Rates expressed by normalizing to the carbon content of the DOM decrease above the threshold value (Table 3).

3.2. Dissolution in Dialysis Experiments

In dialysis experiments designed to impede the contact of F1HpoA with the cinnabar surface, only a small amount of Hg was released from the cinnabar after 9 d. Interior Hg concentrations ranged from 1.77×10^{-8}mol L^{-1} after 2 d to 5.65×10^{-8}mol L^{-1} after 9 d in an experiment with 20 mg C L^{-1} F1HpoA and 10 g L^{-1}HgS. Interior Hg concentrations were almost two orders of magnitude lower than that measured (1.6×10^{-6} mol L^{-1}) after 7 d in a standard dissolution experiment using 20 mg C L^{-1}. Exterior Hg concentrations (in the presence of cinnabar) were small ranging from the detection limit of CVAAS (3×10^{-10} mol L^{-1}) to 2.70×10^{-9} mol L^{-1}. Both interior and exterior Hg concentrations were below the detection limit in the three control experiments which lacked KBr, DOM, or HgS. Minimal DOM was lost by diffusion through the bag during the experiments. Dialysis bags with DOM concentrations of approximately 18 mg C L^{-1} lost an average of 0.6 mg C L^{-1}(<4%), a value which did not change after 2 d and could explain the measurable Hg concentrations outside the bag.

3.3. Sorption of DOM to the Cinnabar Surface

The amount of DOM sorbed to cinnabar in standard experiments ranged from 0.03 to 0.84 mg C m^{-2} (Fig. 4). The error in these concentrations is relatively large (up to ±0.16 mg C m^{-2}) because the standard deviation of duplicate DOC measurements is high (between 0.02 and 0.39 mg C L^{-1}). An inverse relationship between the amount of sorbed DOM and dissolution rate is indicated for the hydrophobic acids (Fig. 4). The fulvic acids show no such relationship within error, but the same trend is suggested if the Pacific Ocean fulvic acid (POFA), the only isolate of marine origin, is not considered. Within error, $SUVA_{280}$ did not change significantly between blanks and reacted samples (Fig. 5), with the exception that $SUVA_{280}$ for Ogeechee River humic acid (OgRHA) increased after reaction. The amount of sorbed DOM for both FIHpoA and WLHpoA increased disproportionately with increasing surface area (Fig. 6) and DOM concentration (Fig. 7). The less dissolution-enhancing isolate, WLHpoA, sorbed to a greater extent than the more dissolution-enhancing isolate F1HpoA. For the data shown in Figure 6, $SUVA_{280}$ values did not change within error (±0.001) as a function of time or surface area.

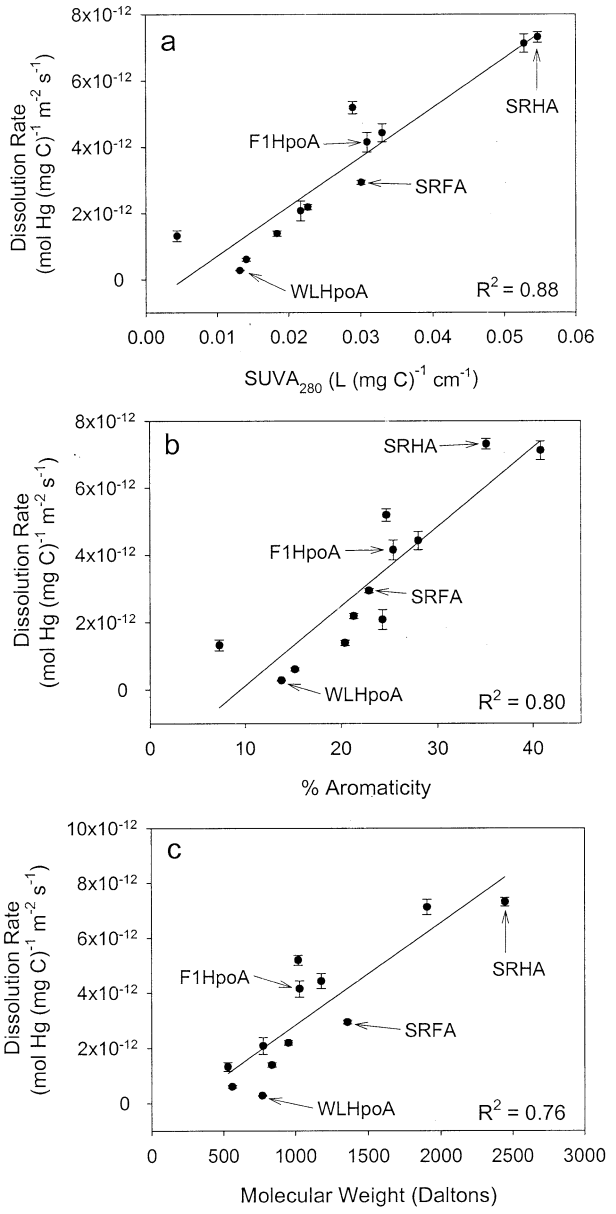

Fig. 2. Dissolution rates vs. properties of the DOM isolates: (a) $SUVA_{280}$ values, (b) per cent aromatic carbon content, and (c) molecular weight. F1HpoA and WLHpoA were used in the dual isolate experiments. SRHA and SRFA are IHSS standards.

3.4. Dissolution Rates in the Presence of Two DOM Isolates

The dissolution rates of cinnabar in the dual isolate experiments (Table 5) were distinct from rates estimated by linear addition of rates in proportion to isolate concentrations. The data in Figure 3 show a linear proportionality for F1HpoA below a threshold ratio of DOM concentration to cinnabar surface area and it was assumed that a similar proportionality existed for WLHpoA. Measured dissolution rates were always greater than the estimated rates for the mixture experiments and lower than the estimated rates for the prereacted replacement experiments. Dissolution rates were always less than the measured rate in the presence of F1HpoA alone, except for the prereacted mixture experiment in which F1HpoA was added before WLHpoA, and the rate was unchanged.

The dissolution rate in the mixture experiment with a 1:1 ratio of WLHpoA and F1HpoA (approximately 5 mg C L^{-1} of each) was 20% lower than the rate in an experiment with only 4.8 mg C L^{-1} F1HpoA (Fig. 8). In contrast, the rate for this mixture was twice the value estimated based on adding 50% by volume of each DOM each reacting at the rates given in Table 3.

In the prereacted mixture experiment in which cinnabar was exposed to WLHpoA before F1HpoA was added, the dissolution rate decreased by 43% compared to that in the F1HpoA dissolution experiment (Tables 3 and 5, Fig. 9a). In contrast, prereacting cinnabar with F1HpoA before adding WLHpoA lowered the rate by only about 5% (Fig. 9b) relative to that in the WLHpoA experiment, which is within the uncertainty of the rate measurement. The rates in these two prereacted mixture experiments also were higher than those estimated for the corresponding simple mixtures, by factors of approximately 1.5 and 2.5, respectively.

In the prereacted replacement experiment in which F1HpoA replaced WLHpoA, the cinnabar dissolution rate was 60% less than the rate in experiments with F1HpoA only (Table 5, Fig. 10a). Replacing WLHpoA with fresh WLHpoA yielded the same reduction in dissolution rate (by 58%) compared to the rate in the experiment with only one added volume of WLHpoA (Table 5, Fig. 10b). These results demonstrate that the effect of WLHpoA in reducing the rate is reproducible and independent of the replacement isolate properties. A 20% rate reduction was observed when fresh F1HpoA replaced an equal amount of the same concentration of F1HpoA (9.3 mg C L^{-1}) and a 42% rate reduction occurred when the concentration of the prereacted F1HpoA (19 mg C L^{-1}) was twice that of the replacement F1HpoA (Fig. 10c). This indicates that the effect on cinnabar dissolution rate is proportional to the concentration of the isolate.

4. DISCUSSION

4.1. Qualitative Dissolution Model

We have shown that the cinnabar dissolution rate is positively correlated to three DOM properties: $SUVA_{280}$, aromaticity, and molecular weight. Results of the dialysis experiments demonstrate that direct interaction between DOM and the HgS surface is needed to promote the dissolution reaction. Because it has been previously established that higher molecular weight and more aromatic DOM sorbs preferentially to oxide minerals (e.g., Meier et al., 1999), we inferred initially that sorption of DOM with higher $SUVA_{280}$, molecular weight, and aromaticity caused the increased dissolution rates. However, we also observed that (1) DOM with lower $SUVA_{280}$ sorbed in greater amounts to cinnabar, (2) dissolution rates for the hydrophobic acids decreased with the amount of DOM sorbed, (3) mixtures of two DOM isolates changed the dissolution rate in a manner that is not simply additive, and (4)

Table 4. Correlations between cinnabar dissolution rates and DOM chemical characteristics.[a]

First characteristic (x_1)	Second characteristic (x_2)	Correlation equation: rate = $ax_1 + bx_2 + c$ a	b	c	R^2
$SUVA_{280}$	—	1.49×10^{-10}		-7.91×10^{-13}	0.88
% Aromatic	—	2.37×10^{-13}		-2.25×10^{-12}	0.80
Molecular weight	—	3.73×10^{-15}		-9.40×10^{-13}	0.76
% Aliphatic I	—	-2.07×10^{-13}		1.10×10^{-11}	0.76
% H	—	-2.40×10^{-12}		1.49×10^{-11}	0.46
% Aliphatic II	—	-5.31×10^{-13}		9.36×10^{-12}	0.40
% O	—	7.06×10^{-13}		-2.33×10^{-11}	0.35
% Ketone	—	4.19×10^{-13}		1.62×10^{-12}	0.23
% Acetal	—	4.29×10^{-13}		1.36×10^{-12}	0.16
% N	—	-1.57×10^{-12}		5.48×10^{-12}	0.16
% S	—	1.50×10^{-12}		1.72×10^{-12}	0.09
% Reduced S[b]	—	6.35×10^{-12}		2.04×10^{-12}	0.19
% C	—	-4.38×10^{-13}		2.69×10^{-11}	0.06
% Carboxyl	—	8.32×10^{-14}		1.62×10^{-12}	0.01
$SUVA_{280}$	% N	1.42×10^{-10}	-6.03×10^{-13}	2.53×10^{-13}	0.90
$SUVA_{280}$	% O	1.40×10^{-10}	1.27×10^{-13}	-5.30×10^{-12}	0.89
$SUVA_{280}$	% S	1.48×10^{-10}	1.01×10^{-13}	-8.68×10^{-13}	0.88
$SUVA_{280}$	% Aliphatic I	1.62×10^{-10}	1.96×10^{-14}	-1.86×10^{-12}	0.88
$SUVA_{280}$	% Aliphatic II	1.50×10^{-10}	4.84×10^{-15}	-8.64×10^{-13}	0.88
$SUVA_{280}$	% Acetal	1.55×10^{-10}	-8.25×10^{-14}	-5.86×10^{-13}	0.88
$SUVA_{280}$	% Carboxyl	1.49×10^{-10}	3.42×10^{-14}	-1.45×10^{-12}	0.88
$SUVA_{280}$	% Ketone	1.50×10^{-10}	1.01×10^{-15}	-7.86×10^{-13}	0.88
$SUVA_{280}$	% Reduced S[b]	1.42×10^{-10}	2.98×10^{-14}	-1.11×10^{-12}	0.89

[a] Rate in units of (mol Hg (mg C)$^{-1}$ m^{-2} s^{-1})
[b] Percentage reduced S is relative to the total mass of DOM.

prereacting cinnabar with one isolate decreased the dissolution rate more than by mere mixing of that isolate with another.

To reconcile these observations, we surmise that neither DOM isolate behaves homogenously with respect to the cinnabar surface. Certain components (for example, separate subsets of molecules or specific functional groups) accelerate and others slow the dissolution rate. Evidence for a surface interaction that increases the dissolution rate exists in the dialysis experiment results that showed that surface contact is necessary to enhance the amount of solubilized Hg. Evidence for a surface interaction that slows the rate comes from the prereacted mixture and replacement experiments.

In a hypothetical dissolution reaction, DOM components sorb to the cinnabar surface and facilitate some change in the coordinative environment of mercury causing the Hg-S bond to break. Mercury is then removed to solution, possibly as a Hg-DOM complex. The sites or functional groups that bind Hg to aqueous DOM are distinct from those sites in the DOM that participate in the rate-limiting step in the dissolution mechanism. Simultaneously, other DOM components sorb irreversibly to the cinnabar surface, alter the surface in a way that reduces subsequent dissolution, and cause the remaining DOM to have different bulk characteristics.

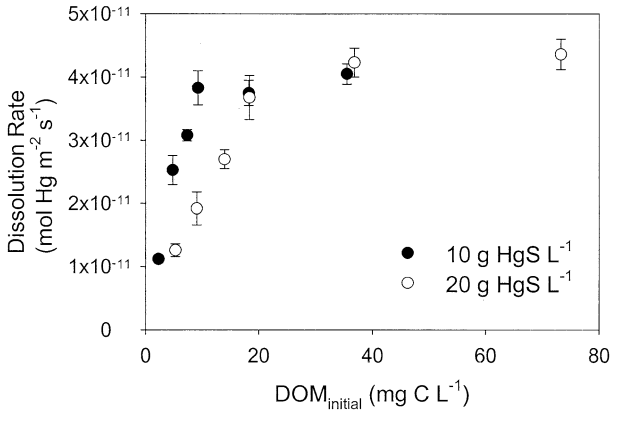

Fig. 3. Variation in dissolution rate with DOM concentration. Dissolution rate approaches a constant value at a threshold concentration of DOM corresponding to 9.2 mg C (g HgS)$^{-1}$.

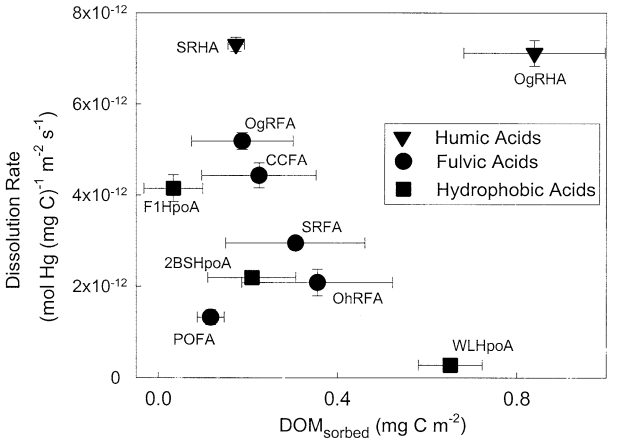

Fig. 4. Dissolution rates vs. the amounts of DOM sorbed to the cinnabar after 10 h.

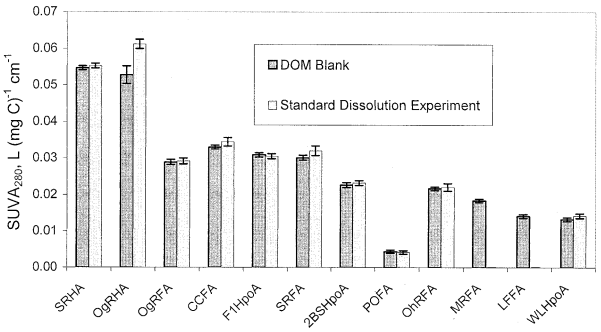

Fig. 5. $SUVA_{280}$ values of the solutions in standard dissolution experiments after 10 h compared to the values in the initial DOM solutions. Measurements were not made on the MRFA and LFFA isolate experiments after reaction.

4.2. Chemical Controls on the Dissolution Rate of Cinnabar

Cinnabar dissolution rates varied by a factor of 26 in the presence of DOM of different origins and this variation correlates with $SUVA_{280}$ of the DOM isolates. Ravichandran et al. (1998) showed a similar result for a limited set of hydrophobic and hydrophilic DOM isolates from one sampling area in the Florida Everglades. In the present study, a correlation with aromaticity ($R^2 = 0.80$) also was observed. Aromaticity is an important indicator of DOM reactivity in a number of processes. For example, high aromaticity increases binding of pyrene (Gauthier et al., 1987), formation of chlorinated byproducts in wastewater (Reckhow et al., 1990), and sorption of DOM to oxide minerals (e.g., Jardine et al., 1989; McKnight et al., 1992; Wang et al., 1997). The correlation with molecular weight ($R^2 = 0.76$) also is consistent with studies of DOM sorption to oxide mineral surfaces indicating that higher molecular weight fractions are adsorbed from solutions with low amounts of DOM and/or during the early stages of sorption (e.g., Meier et al., 1999; Chorover and Amistadi, 2001). Ravichandran et al. (1998) did not observe a correlation between the amount of Hg released from cinnabar after 7 d and molecular weight, but reported a correlation with aromaticity for a subset of their samples. The positive correlations with all three properties in our study suggests that the high molecular weight fraction also is highly aromatic and contains a large percentage of components that absorb light at 280 nm, consistent with the observations of Chin et al. (1994).

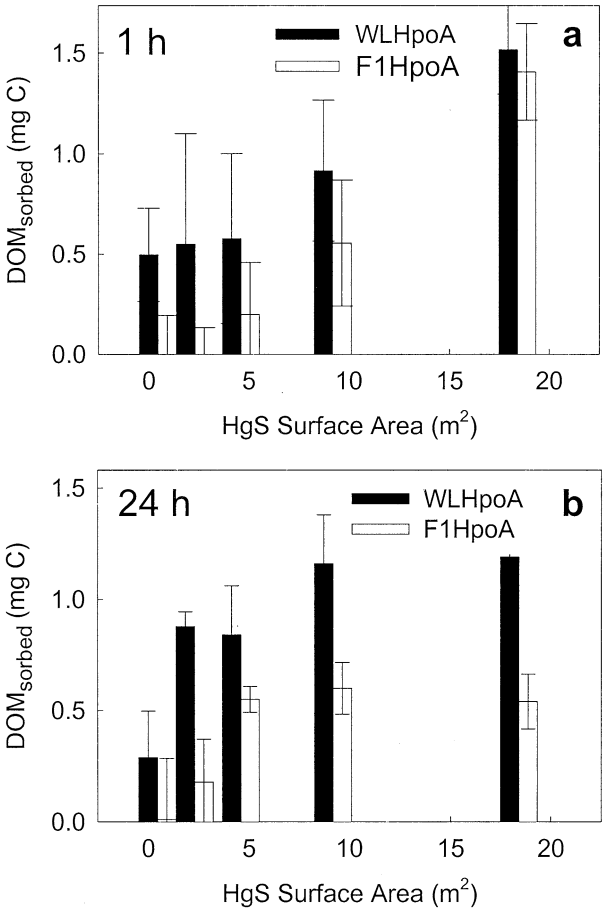

Fig. 6. Amounts of DOM sorbed after (a) 1 h and (b) 24 h as a function of the total surface area of cinnabar for the WLHpoA and F1HpoA isolates. Solutions contained 10 mg C L^{-1} initially and cinnabar concentrations ranged from 2 to 80 g HgS L^{-1}.

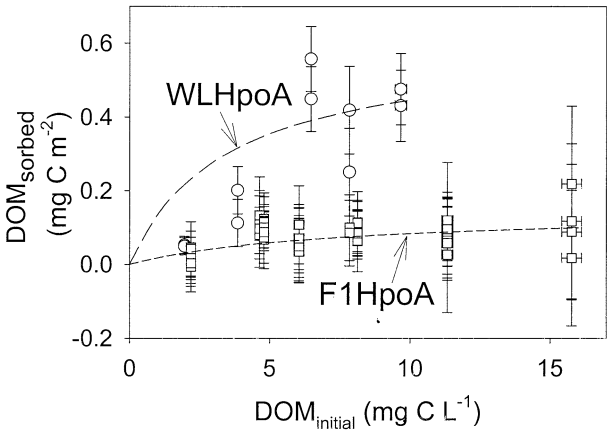

Fig. 7. Amounts of DOM sorbed as a function of the initial solution concentration for the WLHpoA and F1HpoA isolates. Dashed curves are fitted Langmuir isotherms used in an interpretive model of the dissolution mechanism (see Discussion).

In contrast, neither total nor reduced S concentrations correlate with dissolution rate despite the fact that reduced S sites are important for binding Hg to organic matter in solution and in soils (Xia et al., 1999; Skyllberg et al., 2000; Hesterberg et al., 2001). This result agrees with the work of Ravichandran et al. (1998). Thus, interactions of DOM at the cinnabar surface resulting in dissolution do not appear to involve the strongest DOM binding sites. Carboxyl or hydroxyl-bearing functional groups were uncorrelated with the dissolution rates. Low correlations also were observed with every other characterized chemical property of the isolates. It is nonetheless possible that multiple modes of interaction between DOM molecules and the cinnabar surface may have synergistic effects that have not yet been identified.

Cinnabar may dissolve in the presence of the DOM by photocatalysis or oxidation by Fe(III). Photooxidative dissolu-

Table 5. Experimental conditions and dissolution rates for mixture and replacement experiments.

Experiment	Prereacted DOM (mg C L^{-1})[a]	Added DOM (mg C L^{-1})	Total DOM (mg C L^{-1})[b]	Measured dissolution rate (mol Hg (mg C)$^{-1}$ m^{-2} s^{-1})	Estimated[c] dissolution rate (mol Hg (mg C)$^{-1}$ m^{-2} s^{-1})
Mixture		F1HpoA (8.8) WLHpoA (10.2)	9.5	4.19×10^{-12} [d]	2.1×10^{-12}
Prereacted mixture	WLHpoA (10.1)	F1HpoA (9.8)	10.2	3.02×10^{-12}[d]	2.1×10^{-12}
Prereacted mixture	F1HpoA (9.8)	WLHpoA (10.1)	9.7	4.99×10^{-12}[d]	2.1×10^{-12}
Prereacted replacement	WLHpoA (10.2)	F1HpoA (9.3)	10.9	1.66×10^{-12}	3.6×10^{-12}
Prereacted replacement	WLHpoA (10.2)	WLHpoA (9.7)	10.7	1.16×10^{-13}	2.8×10^{-13}
Prereacted replacement	F1HpoA (9.8)	F1HpoA (9.3)	10.8	3.29×10^{-12}	4.2×10^{-12}
Prereacted replacement	F1HpoA (19.0)	F1HpoA (9.3)	11.5	2.40×10^{-12}	4.2×10^{-12}

[a] Measured concentrations in starting solutions.
[b] Measured concentrations at end of experiments.
[c] Calculated using final proportions of the two DOM isolates in each experiment and assuming a linear proportionality between rate and DOM concentration.
[d] Normalized to the DOM concentration of F1 HPoA (approximately one-half the concentration of the mixture DOM).

tion is unlikely because the reactors were shielded from fluorescent laboratory light for most of the experimental duration, and there was no exposure to sunlight. The red cinnabar did not change color to brown (Pal et al., 2003) or black (McCormack, 2000), both of which indicate a photocatalytic reaction at the cinnabar surface. Also, photooxidation did not change the $SUVA_{280}$ values for F1HpoA solution exposed to laboratory light for 15 d. Oxidative dissolution by Fe(III) can enhance the release of Hg to solution from cinnabar (Burkstaller et al., 1975). The Fe(III) content was not determined for all of the DOM sources in Table 1. However, a conservative estimate can be made to assess the likelihood of this mechanism. Fulvic and humic acids from the Suwannee River contain <10 μg/g (below detection) and 200 μg/g Fe, respectively (Taylor and Garbarino, 1994). If all of this iron were soluble, maximum concentrations would have been 4×10^{-9} and 7×10^{-8} mol Fe L^{-1} for SRFA and SRHA, respectively, differing by a factor of 20. The dissolution rate in the presence of SRHA is only 2.5 times, not 20 times, higher than that in the presence of SRFA. Also, these maximum estimates of dissolved Fe are 2.5 to 4 orders of magnitude below the Fe concentration required to release one order of magnitude less Hg to solution from a similar amount of cinnabar surface area in approximately 10 d by comparing to the data reported by Burkstaller et al. (1975). Thus, oxidative dissolution by Fe(III) was probably not a major factor.

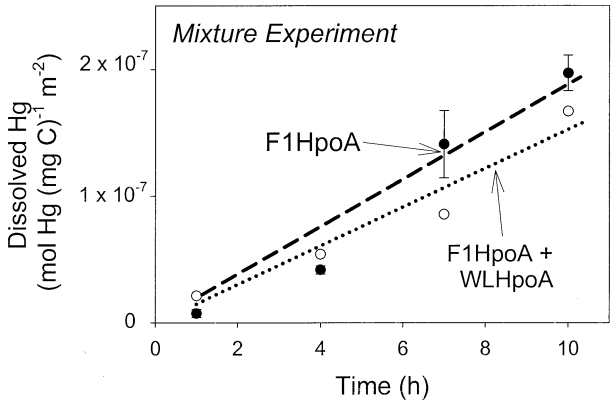

Fig. 8. Normalized concentrations of Hg released from cinnabar (10 g L^{-1}) exposed for 10 h to a mixture of equal amounts of F1HpoA and WLHpoA. Mixture data are compared to those for F1HpoA alone at the same total concentration.

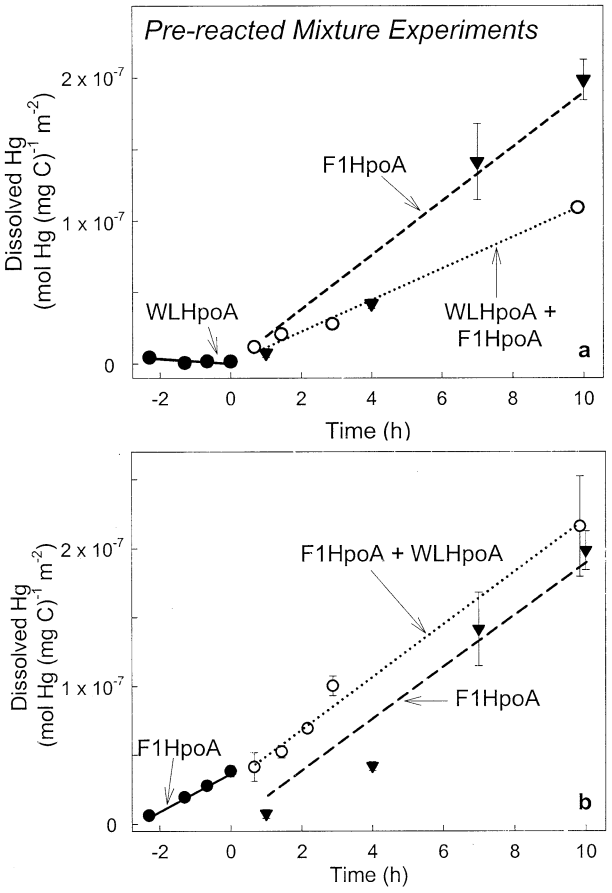

Fig. 9. Normalized concentrations of Hg released from cinnabar (10 g L^{-1}) in prereacted mixture experiments. Negative times indicate the prereaction interval. Positive times indicate reaction after addition of the second DOM isolate. prereacted mixture data are compared to those for F1HpoA alone at the same total concentration. (a) WLHpoA was the first isolate and F1HpoA the second isolate. (b) F1HpoA was the first isolate and WLHpoA the second isolate.

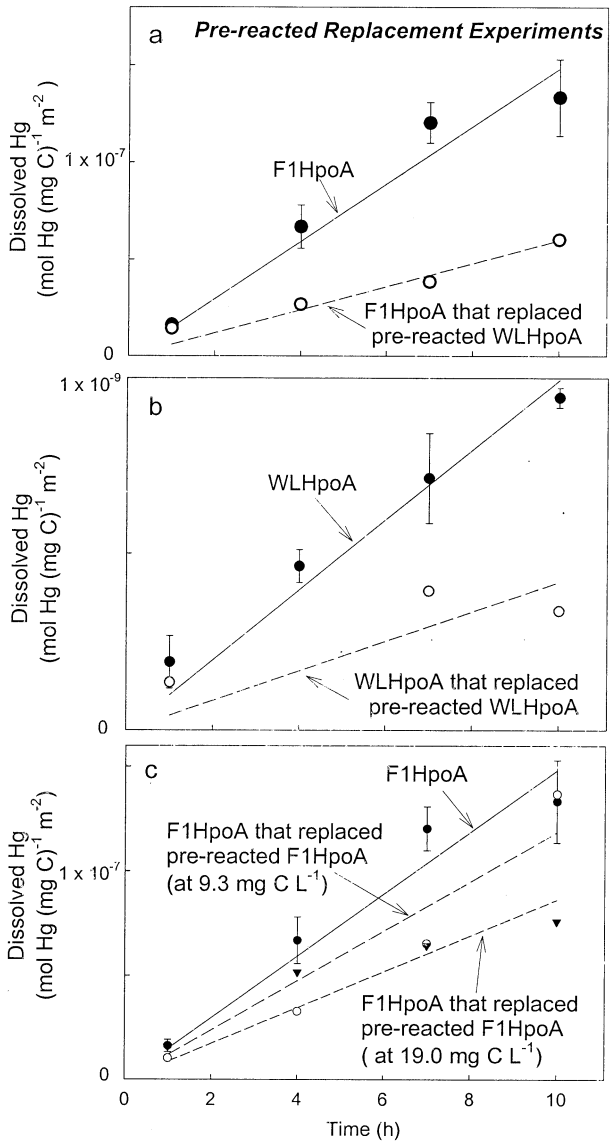

Fig. 10. Normalized concentrations of Hg released from cinnabar (10 g L^{-1}) in prereacted replacement experiments. Data are compared to those for F1HpoA alone at a concentration of 9.3 mg C L^{-1} in (a) and (b) and concentrations of 9.3 and 19.0 mg C L^{-1} in (c). (a) WLHpoA was the first isolate and F1HpoA the second. (b) WLHpoA was the first isolate and WLHpoA the second. (c) F1HpoA was the first isolate and F1HpoA, at concentrations of 9.3 mg C L^{-1} or 19.0 mg C L^{-1}, the second.

4.3. Enhancement of Dissolution via Interaction of DOM with the Cinnabar Surface

The linearity of Hg concentration with time indicates that dissolution in the presence of DOM under far-from-equilibrium conditions follows a zero order rate law, in which rate is a function of specific reactive surface area. Results of the dialysis experiments show that direct contact of DOM with the surface is needed to cause dissolution. The substantially lower amount of Hg observed outside of the dialysis bags at the end of these experiments is likely a result of diffusion of smaller molecular weight components of DOM outward where they could either contact the cinnabar and cause slight dissolution or complex with aqueous Hg released by cinnabar dissolution in the presence of KBr. Diffusion of a mercury-bromide or mercury-bromide-DOM complex inward would explain the concentrations measured from solutions inside the bags (Haitzer et al., 2002), and is consistent with the observation that no detectable Hg was observed in the control experiment containing DOM and no KBr.

Other evidence that a surface sorption step drives cinnabar dissolution is derived from the experiments that showed a threshold rate was reached at a DOM concentration to cinnabar surface area ratio of about 4 mg C m^{-2}. This implies that above some specific surface coverage, the dissolution-enhancing component of DOM cannot promote dissolution because available surface sites are filled. Dissolution can proceed only when Hg is solubilized, freeing a new surface site for interaction with another DOM molecule.

4.4. Slowing of Dissolution via Interaction of DOM with the Cinnabar Surface

For the hydrophobic isolates, there appears to be a strongly sorbed component that slows cinnabar dissolution because rates declined with increasing amounts of sorbed DOM. The correlation between decreasing rate and increasing sorbed DOM provided the impetus to conduct the dual isolate experiments using aliphatic-rich WLHpoA and aromatic-rich F1HpoA as end-member samples (see Table 1). These isolates produced the slowest dissolution rate measured (WLHpoA) and one that was 15 times faster. Thus, this set of experiments was designed to provide some insight into the possibility of competitive sorption between the two isolates.

In the 50–50 mixture experiment, the observed rate was twice as high as expected based on estimating 50% dissolution by each isolate, but was reduced by only 20% compared to the effect of F1HpoA alone, indicating that the two isolates acted independently to cause dissolution and that the F1HpoA isolate controlled the overall dissolution rate. The results of the prereacted mixture experiments support this interpretation. These experiments can be viewed as simple mixtures in which the isolate added first was allowed to react for a longer time and without any interference from the second isolate. When WLHpoA was added first the measured rate was slightly less than that when both isolates were premixed and then added. When F1HpoA was added first, the measured rate was the same as in F1HpoA alone within the uncertainty.

Prereacted replacement experiments differed from the prereacted mixture experiments in two ways. First the absolute amount of the first isolate that was added in the prereacted replacement experiments was twice that added in the prereacted mixture experiments (125 mL of ~ 10 mg C L^{-1} DOM compared to 63 mL of the same concentration solution, respectively). Second, most of the first isolate was removed before adding the second isolate. In all cases, approximately 10–15% of the first isolate remained in the final solution and so the predicted rates were estimated assuming a mixture of approximately 10–15% of the first isolate and 90–85% of the second isolate. Interestingly, all four measured rates were less than the estimated rates. This suggests that the initially higher ratio of DOM to cinnabar surface area was significant in causing more

interference with the dissolution-enhancing reaction. It is inferred that the interference comes from relatively irreversible sorption of components that prevented part of the cinnabar surface from dissolving by interaction with aromatic-rich components.

Removal of components that interfere with the dissolution-enhancing reaction by sorption onto the cinnabar also is supported by results of two one-point standard dissolution experiments that used recycled solutions of DOM. In these separate experiments, 10 g L^{-1} cinnabar was reacted on the rotator with a 9 mg C L^{-1} solution of F1HpoA and a 10 mg C L^{-1} solution of WLHpoA for 20 min, after which the DOM solution was decanted and filtered, and then reused in a new dissolution experiment with fresh cinnabar. Recycled F1HpoA solution released the same amount of Hg after 10 h of reaction, within error, as fresh F1HpoA, but recycled WLHpoA released five times the amount of Hg as fresh WLHpoA (equivalent to an increase in rate of approximately 70%). This implies that the F1HpoA solution did not change significantly after a short period of interaction with cinnabar, but the WLHpoA solution was altered. The change in reactivity of WLHpoA would be consistent with rapid removal of dissolution-slowing components by relatively irreversible sorption onto the cinnabar.

4.5. Nature of Dissolution-Enhancing and Dissolution-Slowing Components of DOM

The dissolution-enhancing component is likely aromatic because faster dissolution rates correlate with higher aromaticity of the DOM. This also suggests the highly aromatic component must interact relatively rapidly with the cinnabar surface to play a role in the dissolution mechanism. The hypothesized dissolution-slowing component functions as a comparatively irreversible sorbate, and is, by inference, deficient in aromatic functional groups. In the dissolution experiments using F1HpoA or WLHpoA with a ratio of DOM to surface area of 4.3 mg C m^{-2} (10 mg C L^{-1} DOM and 10 g HgS L^{-1}) $SUVA_{280}$ values after 10 h did not change significantly from the starting value (Fig. 5). This is consistent with fast sorption of aromatic components, breaking of Hg-S lattice bonds, and return of the aromatic components to solution.

The amount of Hg solubilized by F1HpoA can be used to speculate on the nature of the dissolution-enhancing constituents of the DOM. Hg-release and DOM sorption data from the standard dissolution experiment (i.e., after 10 h of reaction) yield a ratio of dissolved Hg to DOM of 7.5×10^{-2} mol Hg (mol DOM)$^{-1}$ at this stage of reaction. This amount of dissolved Hg per mol of DOM is 15 times greater than the estimated maximum concentration of reduced S binding sites per mol of F1HpoA ($\sim 5 \times 10^{-3}$ mol reduced S (mol DOM)$^{-1}$; Haitzer et al., 2002). This suggests that dissolution is unrelated to direct binding between reduced S functional groups on the DOM and charged sites on the cinnabar surface, which is supported by the lack of correlation between reduced S and dissolution rate. The surface interaction resulting in dissolution may be, for example, a redox-sensitive reaction involving moieties such as quinones.

4.6. Possible Role of Competitive Sorption during Dissolution

We propose a dissolution model based on competitive sorption of dissolution-enhancing and dissolution-slowing components. We assume that WLHpoA represents the dominant dissolution-slowing components and F1HpoA represents the dominant dissolution-enhancing components. F1HpoA likely contains little DOM that slows dissolution because the amount of Hg released after 10 h of reaction did not vary significantly in the single isolate, prereacted replacement (using F1HpoA only), and one-point recycled solution experiments. On the other hand, WLHpoA clearly has components that enhance cinnabar dissolution, but because the dissolution rate was slowed by up to 60% in the dual isolate experiments and apparently enhanced by about 70% after recycling the solution, WLHpoA must contain components that both slow the rate and also sorb more permanently to the cinnabar surface.

If the rate-limiting dissolution reaction depends on DOM sorption to the surface, the rate could be a function of the fraction θ of surface covered by the DOM (Laidler, 1987, p. 244–246):

$$\text{rate} = k\theta = k\frac{K_e[DOM_e]}{1 + K_e[DOM_e] + K_s[DOM_s]} \quad (2)$$

where rate is in units of mol Hg s^{-1}, k is a rate coefficient (mol Hg s^{-1}), K_e and K_s are Langmuir adsorption constants (L (mg C)$^{-1}$) for the dissolution-enhancing and dissolution-slowing components, respectively, and $[DOM_e]$ and $[DOM_s]$ are component concentrations (mg C L^{-1}).

Langmuir adsorption constants were estimated by fitting the isotherm data in Figure 8 to

$$q = q_{max}\frac{K_{DOM}[DOM_{solution}]}{1 + K_{DOM}[DOM_{solution}]} \quad (3)$$

where q is the adsorption density (mg C m^{-2}), q_{max} is the maximum adsorption density assumed to represent monolayer surface coverage, K_{DOM} is the adsorption constant (L mg^{-1} C), and $DOM_{solution}$ is the concentration of dissolved DOM (mg C L^{-1}). Values of $q_{max,F1}$ and K_{F1} were determined directly from the fitted F1HpoA isotherm and equaled 0.14 mg C m^{-2} and 0.14 L (mg C)$^{-1}$, respectively. For the WLHpoA isotherm, we estimated a minimum $q_{max,WL}$at 0.6 mg C m^{-2} (a value just above the highest measured points) and calculated an average value of K_{WL} = 0.29 L (mg C)$^{-1}$, assuming Langmuir-like behavior. True values of K_{DOM} and q_{max} are equivocal because the errors on sorbed DOM concentrations are relatively large, and the isotherms do not show unambiguous plateaus. Nonetheless, the general sense of the data is that WLHpoA sorbs more strongly and to a greater extent than F1HpoA onto cinnabar.

Using the fitted Langmuir adsorption constant for F1HpoA, a value for k equal to 2.26×10^{-12} mol Hg s^{-1} was obtained using Eqn. 2 for the standard dissolution experiment with [F1HpoA] = 4.8 mg C L^{-1} by setting the term for the dissolution-slowing component equal to zero. This k value was then used along with K_e, K_i, and the concentrations of F1HpoA and WLHpoA from the mixture experiment ($[DOM_e]$ = [F1HpoA] = 4.4 mg C L^{-1}; $[DOM_s]$ = [WLHpoA] = 5.1 mg C L^{-1}) and

the WLHpoA-prereacted mixture experiment ([DOM_e] = 4.9 mg C L^{-1} and [DOM_s] = 5.05 mg C L^{-1}) to calculate their rates. Because we don't know the exact concentration and identity of dissolution-enhancing vs. dissolution-slowing components in the DOM, we recast the measured rates in units of mol Hg s^{-1} by factoring out the concentration of F1HpoA, assumed to contain nearly all dissolution-enhancing components. Thus, the measured rates are 9.1×10^{-13} mol Hg s^{-1} for 4.8 mg C L^{-1} of F1HpoA; 6.6×10^{-13} mol Hg s^{-1} for the mixture experiment; and, 5.3×10^{-13} mol Hg s^{-1} for the prereacted mixture experiment using WLHpoA as the first isolate and F1HpoA as the second isolate. For comparison, calculated rates using Eqn. 2 are 4.5×10^{-13} mol Hg s^{-1} for the mixture experiment and 4.9×10^{-13} mol Hg $s^{-1}$for the WLHpoA-prereacted mixture experiment. Model estimates are 70 to 90% of the measured rates. Measured rates are higher than the calculated rates in accordance with the fact that dissolved WLHpoA also contains dissolution-enhancing components. The rate coefficient in Eqn. 2 could be expanded to include explicitly the observed dependence of rate on aromaticity.

Analysis of the DOM components that appear to enhance and slow dissolution as well as additional kinetics experiments are needed to refine the applicability of this type of model. The rates may be minimum rates because Hg(II) has been reported to be readsorbed onto mercury-sulfides during oxidative dissolution (Burkstaller et al., 1975; Barnett et al., 2001). Perhaps readsorbed Hg plays a role in selective adsorption of certain DOM components.

In contrast to previous studies on oxides (Jardine et al., 1989; McKnight et al., 1992; Gu et al., 1994, 1995; Ochs et al., 1994; Wang et al., 1997; Meier et al., 1999; Zhou et al., 2001) and elemental mercury (Ochs et al., 1994) that show preferential sorption of more aromatic and larger molecules, our results indicate that the less aromatic DOM is sorbed preferentially on cinnabar (i.e., WLHpoA sorbs to a greater extent than F1HpoA). Sorption of DOM on oxides is generally assumed to occur through ligand exchange to hydroxylated sites, although the multiplicity of ligand structures may control the extent and strength of sorption (Hering, 1995). Metal sulfides may contain sulfhydryl and hydroxyl surface sites that could be involved in the surface interactions (Rönngren et al., 1991). However, this contrast in behavior may be explained, for example, by the sensitivity of a sulfide or mercury-containing mineral surface to oxidation or reduction reactions influenced by the DOM. Operationally defined DOM fractions, e.g., fulvic, humic, and hydrophobic, represent mixtures of components, and because sorption rates vary (e.g., Gu et al., 1995), attention needs to be paid to specific molecular components of DOM in order to understand fully how DOM affects mineral surface reactivity.

5. CONCLUSIONS

DOM from a variety of natural environments enhances the dissolution of cinnabar to different extents, but always results in dissolved Hg concentrations that are orders of magnitude above those in equilibrium with cinnabar in pure water. Increased Hg solubility has important environmental implications. For instance, concentrations of methylmercury in aquatic systems have been shown to correlate with total dissolved Hg concentrations (Hurley et al., 1995).

Initial rates of dissolution are linearly correlated only to $SUVA_{280}$, aromaticity, and molecular weight of the DOM. Initial rates are independent of the concentration of total or reduced sulfur sites, indicating that direct binding of organic sulfur to Hg is not a controlling factor in the dissolution mechanism. The correlation with aromaticity suggests a role for redox-reaction control of the dissolution mechanism.

Direct interaction between DOM and the cinnabar surface is necessary for the enhanced dissolution. However, evidence for relatively irreversible sorption occurring in parallel was derived from dissolution rate experiments in which two DOM isolates reacted with cinnabar either simultaneously or in sequence and was supported by experiments using recycled DOM solutions. The part of the DOM that remains sorbed during the experiments is inferred to have lower aromaticity and contributes to slowing overall dissolution rates. These results are consistent with a model describing a reduction in cinnabar surface available for dissolution by simple coverage with sorbed DOM that does not tend to enhance dissolution rates (Burkstaller et al., 1975).

Acknowledgments—We acknowledge support from the National Science Foundation's Environmental Geochemistry and Biogeochemistry Program (EAR-9807735) and the U.S. Geological Survey Priority Ecosystems Science Program. We thank Markus Haitzer, Todd Drexel, Jamie Weishaar, and Jarrod Gasper for analytical advice and discussion and Dave Rutherford for the BET analysis. We appreciate the thoughtful comments of three reviewers and the associate editor, which were used in revising the manuscript. Any use of trade, firm, or product names is for descriptive purposes only and does not imply endorsement by the U.S. Government.

Associate editor: G. R. Helz

REFERENCES

Aiken G. R., McKnight D. M., Thorn K. A., and Thurman E. M. (1992) Isolation of hydrophilic organic acids from water using nonionic macroporous resins. *Org. Geochem.* **18,** 567–573.

Aiken G. R., McKnight D. M., Harnish R., and Wershaw R. L. (1996) Geochemistry of aquatic humic substances in the Lake Fryxell Basin, Antarctica. *Biogeochemistry* **34,** 157–188.

Barnett M. O., Harris L. A., Turner R. R., Stevenson R. J., Henson T J., Melton R. C., and Hoffman D. P. (1997) Formation of mercuric sulfide in soil. *Environ. Sci. Technol.* **31,** 3037–3043.

Barnett M. O., Turner R. R., and Singer P. C. (2001) Oxidative dissolution of metacinnabar (β-HgS) by dissolved oxygen. *Appl. Geochem.* **16,** 1499–1512.

Benoit J. M., Gilmour C. C., Mason R. P., and Heyes A. (1999) Sulfide controls on mercury speciation and bioavailability to methylating bacteria in sediment pore waters. *Environ. Sci. Technol.* **33,** 951–957.

Benoit J. M., Mason R. P., Gilmour C. C., and Aiken G. R. (2001) Constants for mercury binding by dissolved organic matter isolates from the Florida Everglades. *Geochim. Cosmochim. Acta* **65,** 4445–4451.

Burkstaller J. E., McCarty P. L., and Parks G. A. (1975) Oxidation of cinnabar by Fe(III) in acid mine waters. *Environ. Sci. Technol.* **9,** 676–678.

Cabaniss S. E., Zhou Q., Maurice P. A., Chin Y., and Aiken G. R. (2000) A log-normal distribution model for the molecular weight of aquatic fulvic acids. *Environ. Sci. Technol.* **34,** 1103–1109.

Chin Y., Aiken G. R., and O'Loughlin E. (1994) Molecular weight, polydispersity, and spectroscopic properties of aquatic humic substances. *Environ. Sci. Technol.* **28,** 1853–1858.

Chin Y., Aiken G. R., and Danielsen K. M. (1997) Binding of pyrene to aquatic and commercial humic substances: The role of molecular weight and aromaticity. *Environ. Sci. Technol.* **37,** 1630–1635.

Chorover J. and Amistadi M. K. (2001) Reaction of forest floor organic matter at goethite, birnessite and smectite surfaces. *Geochim. Cosmochim. Acta* **65,** 95–109.

Compeau G. and Bartha R. (1987) Effect of salinity on mercury-methylating activity of sulfate-reducing bacteria in estuarine sediments. *Appl. Environ. Microbiol.* **53,** 261–265.

Covelli S., Faganeli J., Horvat M., and Brambati A. (2001) Mercury contamination of coastal sediments as the result of long-term cinnabar mining activity (Gulf of Trieste, northern Adriatic Sea). *Appl. Geochem.* **16,** 541–558.

Davis J. A. (1982) Adsorption of natural dissolved organic matter at the oxide/water interface. *Geochim. Cosmochim. Acta* **46,** 2381–2393.

Domagalski J. (2001) Mercury and methylmercury in water and sediment of the Sacramento River Basin, California. *Appl. Geochem.* **16,** 1677–1691.

Driscoll C. T., Yan C., Schofield C. L., Munson R., and Holsapple J. (1994) The mercury cycle and fish in the Adirondack lakes. *Environ. Sci. Technol.* **28,** 136A–143A.

Gauthier T. D., Seitz W. R, Grant C. L. (1987) Effects of structural and compositional variations of dissolved humic materials on pyrene K_{OC} values. *Environ. Sci. Technol.* **21,** 243–248.

Gu B., Schmitt J., Chen Z., Liang L., and McCarthy J. F. (1994) Adsorption and desorption of natural organic matter on iron oxide: Mechanisms and models. *Environ. Sci. Technol.* **28,** 38–46.

Gu B., Schmitt J., Chen Z., Liang L., and McCarthy J. F. (1995) Adsorption and desorption of different organic matter fractions on iron oxide. *Geochim. Cosmochim. Acta* **59,** 219–229.

Gu B., Mehlhorn T. L., Liang L., and McCarthy J. F. (1996) Competitive adsorption, displacement, and transport of organic matter on iron oxide: I. Competitive adsorption. *Geochim. Cosmochim. Acta* **60,** 1943–1950.

Haitzer M., Aiken G. R., and Ryan J. N. (2002) Binding of Mercury(II) to dissolved organic matter: The role of the mercury-to-DOM concentration ratio. *Environ. Sci. Technol.* **36,** 3564–3570.

Hering J. G. (1995) Interaction of organic matter with mineral surfaces: Effects on geochemical processes at the mineral-water interface. In *Aquatic Chemistry: Interfacial and Interspecies Processes* (eds. C. P. Huang, C. R. O'Melia and J. J. Morgan), pp. 95–110. Advances in Chemistry Series 244. American Chemical Society.

Hesterberg D., Chou J. W., Hutchison K. J., and Sayers D. J. (2001) Bonding of Hg(II) to reduced organic sulfur in humic acid as affected by S/Hg ratio. *Environ. Sci. Technol.* **35,** 2741–2745.

Hsu H. and Sedlak D. L. (2003) Strong Hg(II) complexation in municipal wastewater effluent and surface water. *Environ. Sci. Technol.* **37,** 2743–2749.

Huffman E. W. D and Stuber H. A. (1985) Analytical methodology for elemental analysis of humic substances. In *Humic Substances in Soil, Sediment, and Water: Geochemistry, Isolation, and Characterization* (eds. G. R. Aiken, D. M. McKnight and R. L. Wershaw), pp. 433–456. Wiley.

Hurley J. P., Benoit J. M., Babiarz C. L., Shafer M. M., Andren A. W., Sullivan J. R., Hammond R., and Webb D. A. (1995) Influences of watershed characteristics on mercury levels in Wisconsin rivers. *Environ. Sci. Technol.* **29,** 1867–1875.

Hurley J. P., Krabbenhoft D. P., Cleckner L. B., Olson M. L., Aiken G. R., and Rawlik P. S. Jr. (1998) System controls on the aqueous distribution of mercury in the northern Everglades. *Biogeochemistry* **40,** 293–311.

Jardine P. M., Weber N. L., and McCarthy J. F. (1989) Mechanisms of dissolved organic carbon adsorption on soil. *Soil Sci. Soc. Am. J.* **53,** 1378–1385.

Krabbenhoft D. P. and Babiarz C. (1992) The role of groundwater transport in aquatic mercury cycling, *Water Resources Res.* **12,** 3119–3128.

Krabbenhoft D. P., Hurley J. P., Aiken G., Gilmour C., Marvin-DiPasquale M., Orem W. H., and Harris R. (2000) Mercury cycling in the Florida Everglades: A mechanistic field study. *Verh. Internat. Verein. Limnol.* **27,** 1657–1660.

Laidler K. J. (1987) *Chemical Kinetics.* Harper and Row.

Lamborg C. H., Tseng C.-M., Fitzgerald W. F., Balcom P. H., and Hammerschmidt C. R. (2003) Determination of the mercury complexation characteristics of dissolved organic matter in natural waters with "reducible Hg" titrations. *Environ. Sci. Technol.* **37,** 3316–3322.

Martell, A. E. and Smith, R. M. (1998) *Critically Selected Stability Constants of Metal Complexes Database Version 5.0.* National Institute of Standards and Technology.

McCormack J. K. (2000) The darkening of cinnabar in sunlight. *Min. Dep.* **35,** 796–798.

McKnight D. M., Bencala K E., Zellweger G. W., Aiken G. R., Feder G. L., and Thorn K. A. (1992) Sorption of dissolved organic carbon by hydrous aluminum and iron oxides occurring at the confluence of Deer Creek with the Snake River, Summit County, Colorado. *Environ. Sci. Technol.* **26,** 1388–1396.

Meier M., Namjesnik-Dejanovic K., Maurice P. A., Chin Y.-P., and Aiken G. R. (1999) Fractionation of aquatic natural organic matter upon sorption to goethite and kaolinite. *Chem. Geol.* **157,** 275–284.

Meili M. (1991) The coupling of mercury and organic matter in the biogeochemical cycle—Towards a mechanistic model for the boreal forest zone. *Water Air Soil Pollut.* **56,** 333–348.

Ochs M., Cosovic B., and Stumm W. (1994) Coordinative and hydrophobic interaction of humic substances with hydrophilic Al_2O_3 and hydrophobic mercury surfaces. *Geochim. Cosmochim. Acta* **58,** 639–650.

Pal B., Ikeda S., and Ohtani B. (2003) Photoinduced chemical reactions on natural single crystals and synthesized crystallites of mercury(II) sulfide in aqueous solution containing naturally occurring amino acids. *Inorganic Chem.* **42,** 1518–1524.

Ravichandran M. (1999) Interactions between mercury and dissolved organic matter in the Florida Everglades. Ph.D. thesis, Univ. of Colorado.

Ravichandran M. (2004) Interactions between mercury and dissolved organic matter—A review. *Chemosphere* **55,** 319–331.

Ravichandran M., Aiken G. R., Reddy M. M., and Ryan J. N. (1998) Enhanced dissolution of cinnabar (mercury sulfide) by dissolved organic matter isolated from the Florida Everglades. *Environ. Sci. Technol.* **32,** 3305–3311.

Ravichandran M., Aiken G. R., Reddy M. M., and Ryan J. N. (1999) Inhibition of precipitation and aggregation of metacinnabar (mercuric sulfide) by dissolved organic matter from the Florida Everglades. *Environ. Sci. Technol.* **33,** 1418–1423.

Reckhow D. A., Singer P. C., and Malcolm R. L. (1990) Chlorination of humic materials: Byproduct formation and chemical interpretations, *Environ. Sci. Technol.* **24,** 1655–1664.

Reddy M. M. and Aiken G. R. (2001) Fulvic acid-sulfide binding competition for mercury ion binding in the Florida Everglades. *Water Air Soil Pollut.* **132,** 89–104.

Rönngren L, Sjöber S., Sun Z., Forsling W., and Schindler P. W. (1991) Surface reactions in aqueous metal sulfide systems. *J. Colloid Interface Sci.* **145,** 396–404.

Shanley J. B., Schuster P. A., Reddy M. M., Roth D. A., Taylor H. E., Aiken G. R. (2002) Mercury on the move during snowmelt in Vermont. *Eos* **83,** 45–48.

Skyllberg U., Xia K., Bloom P., Nater E. A., and Bleam W. F. (2000) Binding of mercury (II) to reduced sulfur in soil organic matter along upland-peat soil transects. *J. Environ. Qual.* **29,** 855–865.

Taylor H. E. and Garbarino J. R. (1994) Occurrence and distribution of selected trace metals in the International Humic Substances Society's standard and reference fulvic and humic acids isolated from the Suwannee River. In *Humic Substances in the Suwannee River, Georgia: Interactions, Properties and Proposed Structures* (eds. R. C. Averett, J. L. Leenheer, D. M. McKnight and K. A. Thorn), pp. 45–54. Water Supply Paper 2373. U.S. Geological Survey.

Vairavamurthy M. A., Maletic D., Wang S., Manowitz B., Eglinton T., and Lyons T. (1997) Characterization of sulfur-containing functional groups in sedimentary humic substances by X-ray absorption near-edge spectroscopy. *Energy Fuels* **11,** 546–553.

Wang L., Chin Y.-P., and Traina S. J. (1997) Adsorption of (poly)maleic acid and an aquatic fulvic acid by goethite. *Geochim. Cosmochim. Acta* **61,** 5313–5324.

Weishaar J. L., Aiken G. R., Bergamaschi B. A., Fram M. S., Fujii R., and Mopper K. (2003) Evaluation of specific ultraviolet absorbance as an indicator of the chemical composition and reactivity of dissolved organic carbon. *Environ. Sci. Technol.* **37,** 4702–4708.

Wershaw R. L. (1985) Application of nuclear magnetic resonance spectroscopy for determining functionality in humic substances. In *Humic Substances in Soil, Sediment, and Water: Geochemistry, Isolation, and Characterization* (eds. G. R. Aiken, D. M. McKnight and R. L. Wershaw), pp. 561–582. Wiley.

Xia K., Skyllberg U. L, Bleam W. F., Bloom P. R., Nater E. A., and Helmke P. A. (1999) X-ray adsorption spectroscopic evidence for the complexation of Hg(II) by reduced sulfur in soil humic substances. *Environ. Sci. Technol.* **33,** 257–261.

Zhou Q., Maurice P. A., and Cabaniss S. E. (2001) Size fractionation upon adsorption of fulvic acid on goethite: Equilibrium and kinetic studies. *Geochim. Cosmochim Acta* **65,** 803–812.